A theoretical study of half-metallic antiferromagnetic diluted magnetic semiconductors

2007 J. Phys.: Condens. Matter 19 216220

(http://iopscience.iop.org/0953-8984/19/21/216220)

IOP PUBLISHING JOURNAL OF PHYSICS: CONDENSED MATTER

J. Phys.: Condens. Matter **19** (2007) 216220 (14pp) doi:10.1088/0953-8984/19/21/216220

A theoretical study of half-metallic antiferromagnetic diluted magnetic semiconductors

L Bergqvist and P H Dederichs

Institut für Festkörperforschung, Forschungszentrum Jülich, D-52425 Jülich, Germany

Received 28 February 2007, in final form 1 March 2007
Published 2 May 2007
Online at stacks.iop.org/JPhysCM/19/216220

Abstract

Based on electronic structure calculations and statistical methods, we investigate a new class of materials for spintronic applications: half-metallic antiferromagnetic diluted magnetic semiconductors (HMAF-DMSs). As shown recently by Akai and Ogura, these DMS systems contain equal amounts of low-valent and high-valent transition metal impurities, such that their local moments exactly compensate each other. We present *ab initio* calculations using the KKR-CPA and the PAW-supercell methods, and show that quite a few half-metallic antiferromagnets should exist. Our calculations demonstrate that the exchange coupling parameters in these systems are dominated by a strong antiferromagnetic interaction between the two impurities. The Néel temperatures are calculated by Monte Carlo simulations and in mean-field approximation. It is shown that the latter method strongly overestimates the critical temperatures and that the more realistic values obtained by Monte Carlo techniques are rather low.

(Some figures in this article are in colour only in the electronic version)

1. Introduction

In recent years, there has been a great interest in various materials aimed for applications in spintronics [1–3]. Combining the electronic charge and spin degrees of freedom opens up the possibility for materials with new functionality. This includes magnetic multilayers which are used in giant magnetoresistance read-heads in hard disks, diluted magnetic semiconductors (DMSs) and half-metallic ferromagnets like Heusler alloys. In particular, DMS systems have attracted lots of attention [4–7], both theoretically and experimentally, ever since the discovery of large-T_c ferromagnetism in Mn-doped GaAs by Ohno in 1998 [3]. In the last few years, more sophisticated control over defects in the samples and annealing have increased the critical temperature, T_c, from around 110 K to around 175 K for Mn-doped GaAs. Still, the T_c is well below room temperature, which prohibits a practical use of this material for devices. Many other systems have been suggested to have room-temperature ferromagnetism, including the III–V systems GaP [8] and GaN [9, 10] doped with Mn, the II–VI system ZnTe doped with

Cr [11] and Co-doped ZnO [12, 13]. Maybe the II–VI systems are the most promising due to the fact that the solubility of magnetic transition metal atoms is much higher than for III–V systems. However, in all these studies one comes to the conclusion that the critical temperatures are very dependent on the sample preparation, the number of (non-magnetic) defects and possible clustering of the magnetic atoms.

Recently, Akai and Ogura [14] proposed some new form of DMS systems, i.e. half-metallic antiferromagnetic diluted magnetic semiconductors. They are very different from the standard ferromagnetic or disordered-local-moment (DLM) phases of DMSs. Necessarily, they contain equal concentrations of two kinds of impurity, e.g. Cr and Fe in $Zn_{1-2x}Cr_xFe_xSe$, such that the moments of these impurities, i.e. of Cr and Fe, are equal and exactly compensate each other by antiparallel alignment. To obtain half-metallicity, it is essential that both impurities are chemically different. Note that in an elemental antiferromagnet the density of states for the two sublattices differs only by an exchange of the spin directions, such that the total density of states is the same for both spin directions. Therefore elemental antiferromagnets are either metals or insulators, but cannot be half-metals, which have a 100% spin polarization at the Fermi level being essential for spintronics.

The possible existence of half-metallic antiferromagnets was first pointed out by van Leuken and de Groot [15], who proposed CrMnSb and $V_{0.875}Mn_{0.125}FeSb_{0.875}In_{0.125}$ as candidates for half-metallicity. Later, Pickett [16] showed by *ab initio* calculations that the double perovskites La_2VCuO_6, La_2MnO_6 and La_2MnCoO_6 are also candidates for half-metallic antiferromagnets. However, experimentally neither of these candidates have been confirmed and it is likely that the considered magnetic crystal structures are not thermodynamically stable. Since by molecular beam epitaxy many thermodynamically unstable systems can be produced, we consider it likely that the proposed half-metallic antiferromagnetic DMSs can be realized in the future.

In this paper we give an extensive discussion of half-metallic antiferromagnetic DMS systems. Firstly we discuss some simple sum rules connecting the moments and the valences of antiferromagnetic and ferrimagnetic half-metallic DMSs. In the latter cases the moments of the two subsystems are also aligned antiparallel, but they are only partially compensated, such that the moment of an impurity pair is a finite integer number. Then we present ground-state calculations for the antiferromagnetic systems $Zn_{1-2x}Cr_xFe_xSe$ and $Zn_{1-2x}V_xCo_xSe$. We show that, for III–V semiconductors, antiferromagnetic DMSs with half-metallic behaviour do not exist in GaAs, but are more likely to exist in wide band gap semiconductors like GaN. In the *ab initio* calculations we use the KKR-CPA method as well as the PAW method as implemented in the VASP code [17, 18]. In this supercell method the disorder is described by special quasirandom structures (SQSs). Both methods give very similar results. Then we calculate the exchange coupling constants between the different impurity pairs and calculate the Néel temperatures of the antiferromagnetic systems and the Curie temperatures of the ferrimagnetic ones by Monte Carlo simulations. Due to the short range of the exchange couplings the critical temperatures of these systems are strongly reduced as compared to the mean-field estimates. This is quite analogous to recent findings [19–22] that percolation effects strongly reduce the Curie temperatures of 'elemental' DMSs like (Ga, Mn)N or (Zn, Cr)Te.

2. Theory

2.1. Simple sum rules

Here we derive some simple sum rules connecting the total moments and the charges for half-metallic systems. These sum rules are the result of simply counting the number of occupied

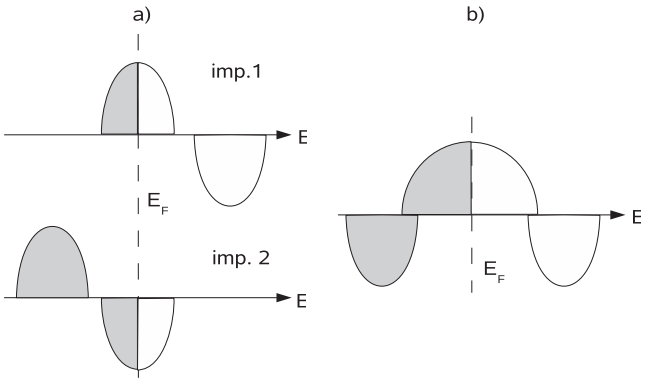

Figure 1. (a) Schematic DOS of the impurity bands of a low-valent impurity 1 and of a high-valent impurity 2 in a DMS. (b) Schematic DOS of the impurity states in a half-metallic antiferromagnet. Impurities 1 and 2 are aligned antiparallel and form a joint impurity band at E_F.

states in the system, and are always valid, if the system is half-metallic. For instance, they do not change if the LDA or the LDA + U approximation is used. However, the state counting only yields the total moments, not the local ones, which in fact are in a LDA + U treatment sensitive to the U-values chosen. Following the arguments of Akai and Ogura [14], figure 1(a) shows schematically the density of states in the gap of a dilute magnetic semiconductor. The first figure shows the density of states (DOS) for a low-valent impurity 1 with partially occupied majority states, while the second figure shows the analogous DOS for a higher-valent impurity 2, for which the majority states are fully and the minority states partially occupied. The total moments M_1 and M_2 are related to the total valence charges Z_1 and Z_2 as $M_1 = \Delta Z_1$ with $\Delta Z_1 = Z_1 - N_{VB}$ for $0 \leqslant \Delta Z_1 \leqslant 5$ and $M_2 = 10 - \Delta Z_2$ with $\Delta Z_2 = Z_2 - N_{VB}$ for $5 \leqslant \Delta Z_2 \leqslant 10$ provided the systems are half-metallic. N_{VB} is the number of valence electrons of the substituted atom. For instance, for impurities on a III-site in a III–V compound semiconductor $N_{VB} = 3$, since three electrons of the impurity are needed to fill up the valence band, so that only the remaining ΔZ electrons can form the moment. As an example, in (Ga, Mn) three of the seven Mn electrons fill up the valence band states, substituting for the three Ga electrons, and the four remaining electrons form the total magnetic moment of 4 μ_B.

As shown in [14], a half-metallic antiferromagnetic DMS can be found by doping with equal numbers of low-valent and high-valent impurities. The antiferromagnetic configuration exhibits a characteristic DOS shown in figure 1(b), where the partially occupied majority band of impurity 1 lines up with the partially occupied minority band of impurity 2 to form a joint band at E_F, which stabilizes the antiferromagnetic configuration by double exchange. The integer total moment M_T of the pair in the case of half-metallicity is given by $M_T = \Delta Z_1 + \Delta Z_2 - 10 = Z_1 + Z_2 - 10 - 2N_{VB}$ since the available electrons for the impurity bands fill up first the five lower-lying majority states of impurity 2, while the remaining electrons fill up the joint band at E_F. A half-metallic antiferromagnet with vanishing moment $M_T = 0$ can exist if $\Delta Z_1 + \Delta Z_2 - 10 = 0$ or $Z_1 + Z_2 = 10 + 2N_{VB}$. For impurities on the III-site in III–V compounds this condition is $Z_1 + Z_2 = 16$, while for impurities on the II-site in II–VI semiconductors $Z_1 + Z_2 = 14$ must be satisfied. Thus only the following combinations are possible candidates for half-metallic antiferromagnets:

II site in II–VI: Cr–Fe, V–Co and Ti–Ni

III site in III–V: Mn–Co and Cr–Ni.

Other combinations with antiparallel alignment can exist; however, the total moment M_T is not fully compensated and has an integer value $M_T = \pm 1, \pm 2, \ldots$. These systems are then half-metallic ferrimagnetic DMSs. For instance, such ferrimagnetic systems with $M_T = \pm 1$ could be $Zn_{1-2x}Cr_xCo_xSe$ or $Ga_{1-2x}Mn_xFe_xAs$. Of course, many more ferrimagnetic combinations can exist.

2.2. Electronic structure

The electronic structure calculations were performed using two complementary methods. The main body of the calculations was performed using the Korringa–Kohn–Rostoker (KKR) Green's function method in the multipole-corrected atomic sphere approximation (ASA+M) [23]. Empty spheres were included in the tetrahedral positions of the zinc blende lattice in order to obtain good space-filling. Equal Wigner–Seitz radii were used for all spheres, and the valence basis set consists of spdf orbitals where scalar relativistic corrections are taken into account while spin–orbit effects are neglected. The effects of disorder were treated in the framework of the coherent potential approximation (CPA). The local spin density approximation was employed for the exchange–correlation potential by using the parameterization of Perdew *et al* [24].

In order to check the accuracy of the CPA and ASA we have also performed supercell calculations using the projector augmented wave (PAW) method as implemented in the Vienna *ab initio* simulation package (VASP) [17, 18]. A energy cutoff of 350 eV was employed and both the local spin density approximation (LSDA) and the LSDA $+$ U method were considered. In the LSDA $+$ U calculations, the value of the Hubbard U parameter was fixed to $U = 3$ eV and the exchange to $J = 0.8$ eV and was included on the d states of the magnetic atoms. Disorder was taken into account by employing so-called special quasirandom structures (SQSs) [25]. The SQS scheme is a method to create as good supercells as possible on random disordered systems by minimizing the chemical short-range parameters. The quality of such minimization depends of course of the size of the supercell. In the present calculations a 128-atom supercell (a $4 \times 4 \times 4$ zinc blende lattice) was used in which a total of six magnetic atoms were included (three of each kind). This corresponds to a concentration $x = 4.7\%$. A larger supercell consisting in total of 250 atoms of which 12 were magnetic atoms (six of each kind) was tested, but this did not yield any significant changes of the results compared to the 128 atom supercell.

2.3. Exchange interactions

The classical multicomponent Heisenberg Hamiltonian in zero external magnetic field can be written in the following form:

$$H = -\sum_{ij,QQ'} J_{ij}^{QQ'} \mathbf{e}_i^Q \cdot \mathbf{e}_j^{Q'}, \tag{1}$$

where $J_{ij}^{QQ'}$ are exchange interactions, i, j are unit cell indices, Q, Q' are atom type indices and $\mathbf{e}_i^Q$ is the unit vector parallel to the magnetization at the site i with atomic type Q. The positive (negative) values of $J_{ij}^{QQ'}$ correspond to the ferromagnetic (antiferromagnetic) couplings, respectively, and the magnitudes of the corresponding magnetic moments are included in the definition of $J_{ij}^{QQ'}$. The exchange interactions were obtained by mapping the electronic structure calculations to the classical Heisenberg Hamiltonian. Here we employ the magnetic force theorem to calculate the energy change due to small rotation of the moment directions of

the atoms at sites i and j [26]. In the framework of KKR–ASA–CPA the energy change could then be related to the exchange interaction by

$$\bar{J}_{ij}^{Q,Q'} = -\frac{1}{8\pi i}\int_C \mathrm{Tr}_L\left[\Delta_i^Q(z)\bar{g}_{ij}^{QQ',\uparrow}(z)\Delta_j^{Q'}(z)\bar{g}_{ji}^{Q'Q,\downarrow}(z)\right]\mathrm{d}z. \tag{2}$$

Here Tr_L denotes the trace over the angular momentum $L = (\ell m)$, $\Delta_i^Q(z) = P_i^{Q,\uparrow}(z) - P_i^{Q,\downarrow}(z)$ is a diagonal matrix defined via the potential functions $P_i^{Q,\sigma}(z)$ and is closely related to the exchange splitting corresponding to the magnetic atom Q, and $\bar{g}_{ij}^{QQ',\uparrow}(z)$ and $\bar{g}_{ji}^{Q'Q,\downarrow}(z)$ refer to site off-diagonal blocks of the conditionally averaged Green function, namely the average over all configurations with a pair of magnetic atoms fixed at the sites i and j with the components Q and Q'. The energy integration is performed along a contour in the complex energy plane which encircles the occupied part of the valence band. It should be noted that the present formalism neglects local environment effects of the exchange interactions, the so-called plurality effect [27], which can only be accounted for using supercells.

2.4. Critical temperatures

The critical temperatures were evaluated using both the mean-field approximation (MFA) and the more sophisticated Monte Carlo (MC) simulations. In the MFA, the critical (Néel) temperature, T_N, can be estimated in two ways. First, T_N is proportional to the total energy difference between the antiferromagnetic ground state and the disordered local moment (DLM) configuration. The DLM state can be naturally treated in the framework of the CPA: the magnetic atoms have collinear but random positive and negative orientations. For instance, the $Zn_{1-2x}Mn_xFe_xSe$ alloy is treated as $Zn_{1-2x}Mn^+_{x/2}Mn^-_{x/2}Fe^+_{x/2}Fe^-_{x/2}Se$ in the DLM configuration. T_N can then be estimated using the following expression:

$$k_\mathrm{B}T_\mathrm{N}^{*\mathrm{MFA}} = \frac{2}{3}\frac{(E_\mathrm{DLM} - E_\mathrm{AF})}{c}, \tag{3}$$

where E_DLM and E_AF are the total energies for the DLM and AF configurations, respectively, c is the total concentration of magnetic atoms ($c = 2x$) and k_B is the Boltzmann constant. Alternatively, the mean-field estimate of T_N can be estimated from the exchange interactions $J_{ij}^{QQ'}$ [28, 29]. More specifically, T_N is related to an eigenvalue problem of the real symmetric matrix $\mathbb{J}(\mathbf{0})$ with elements $J^{QQ'}(\mathbf{0})$: namely,

$$\sum_{Q'} J^{QQ'}(\mathbf{0})\langle e_z^{Q'}\rangle = \frac{3k_\mathrm{B}T^\mathrm{MFA}}{2}\langle e_z^Q\rangle, \tag{4}$$

$$J^{QQ'}(\mathbf{0}) = x\sum_j J_{0j}^{QQ'}, \tag{5}$$

where $\langle e_z^Q\rangle$ is the thermodynamically averaged z component of the unit vector $\mathbf{e}_i^Q$. The Néel temperature, $T_\mathrm{N}^\mathrm{MFA}$, and the Curie temperature, T_C^MFA, respectively, is then given by the highest of the two eigenvalues T^MFA of the $2\times 2\,\mathbb{J}(\mathbf{0})$ matrix. In principle, the expression using the total energy difference is more accurate since all exchange interactions in the system are taken into account. Moreover, the vertex corrections to the exchange interactions cancel exactly. It should be noted that the above expressions employ the so-called virtual crystal approximation (VCA) or the averaged lattice in order to deal with diluted magnetic systems. It is known from earlier studies [19–22] that this approximation is very bad for diluted systems with localized exchange interactions where disorder and percolation effects play an important role. Therefore we have also evaluated T_N using Monte Carlo simulations where both disorder and thermal fluctuations are included in a numerically exact procedure. The MC simulations employed

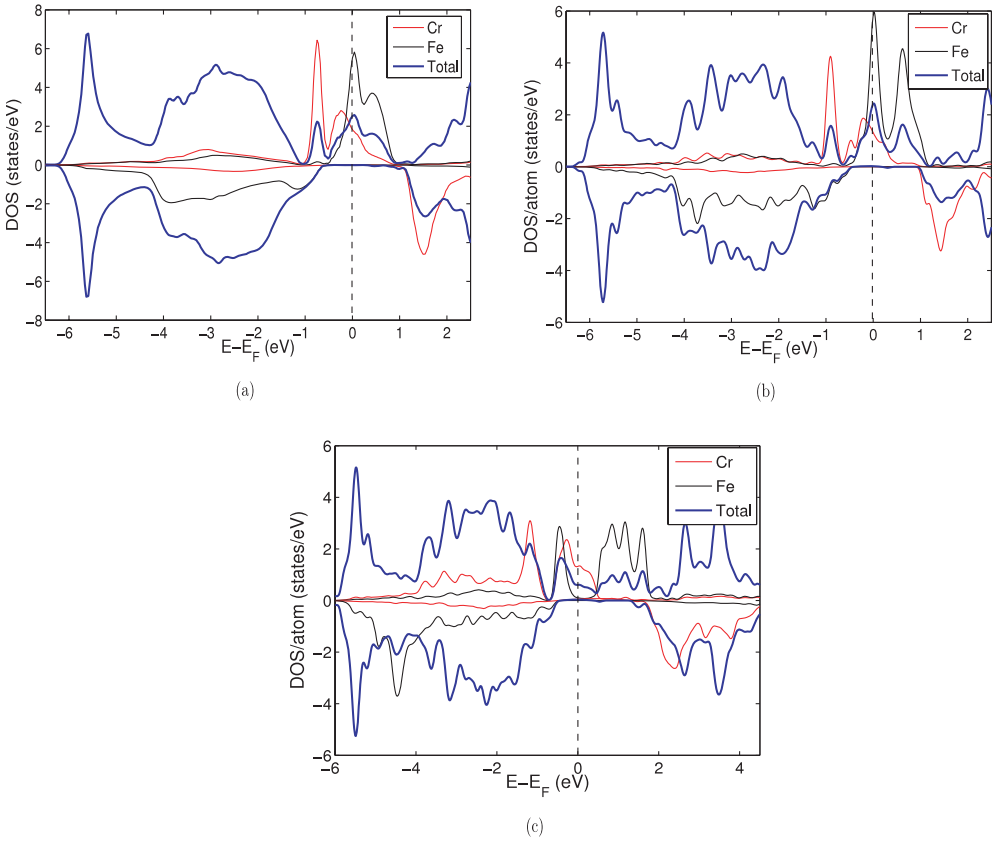

Figure 2. Density of states (DOS) of $Zn_{0.9}Cr_{0.05}Fe_{0.05}Se$ using the (a) KKR-ASA method (LDA), (b) PAW method (LDA) and (c) PAW method (LDA + U). Positive (negative) values correspond to majority (minority) states. The total DOS has been scaled for better readability.

the Metropolis algorithm in which the critical temperature was evaluated from the peak in some thermodynamic quantities (susceptibility and the specific heat) for the antiferromagnetic systems. In the case of ferrimagnetic systems the critical temperature was evaluated by means of the cumulant crossing method [30]. In all cases the lattice size was varied in order to employ finite size scaling and the total number of magnetic atoms in the system was varied between 10 000 and 40 000. Ten disorder configurations were realized for each lattice size and the thermal average of the magnetization was measured for around 30 000 Monte Carlo steps per lattice site.

3. Results

3.1. Antiferromagnetic solutions

In all following results on the doped II–VI materials we use ZnSe as the semiconductor host material and GaAs for the III–V systems. We believe that the results for ZnSe are typical also for other II–VI semiconductors. The experimental lattice constant was used in all calculations.

3.1.1. Density of states and magnetic moments. In figure 2 the calculated density of states of $Zn_{0.9}Cr_{0.05}Fe_{0.05}Se$ is displayed. The CPA calculations (figure 2(a)), and supercell PAW

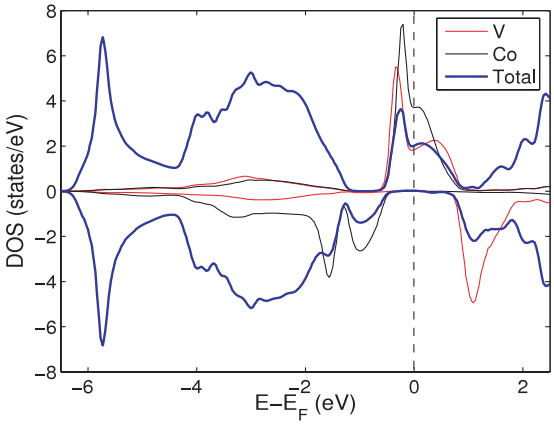

Figure 3. Density of states (DOS) of $Zn_{0.90}V_{0.05}Co_{0.05}Se$ using the KKR-ASA method (LDA). Positive (negative) values correspond to majority (minority) states. The total DOS has been scaled for better readability.

calculations (figure 2(b)) using the LDA agree well with each other and also agree well with the CPA calculations in [14]. The PAW calculations show slightly more features in the DOS due to the smaller smearing used in the calculations compared to the CPA calculations. A half-metallic ground state is found with zero total magnetic moment. The average local magnetic moment on Cr and Fe was found to be 3.48 and $-3.26\ \mu_B$ in the KKR calculation. The corresponding values in the PAW calculations were 3.41 and $-3.15\ \mu_B$. Note that in the PAW method these values refer to the moments inside a sphere surrounding each atom. The moments should be compared with the total moment of 4 μ_B per impurity for the ferromagnetic (Zn, Cr)Se and (Zn, Fe)Se systems (however, the local magnetic moments are basically the same). The fact that we have small induced magnetic moments in the interstitial region and on the Zn and Se atoms, and the fact that the system is half-metallic, make the total magnetic moment to average to zero (integer number) in the whole cell. Around the Fermi level a common impurity band in the spin-up channel originating from the Cr and Fe d states is clearly present and is well understood from hybridization. The hybridization of these states lowers the band energy and also determines the magnetic coupling of the system.

The effect of electron correlations using the LDA + U method is displayed in figure 2(c). The effect on the electronic structure is briefly the following: it causes an additional splitting of the states, and the band gap in the spin-down channel increases. The local magnetic moments also slightly increase compared with the LDA values, which is rather typical for transition metals.

In figure 3 a similar plot of the calculated DOS of $Zn_{0.9}V_{0.05}Co_{0.05}Se$ is displayed using the KKR-CPA method. The electronic structure is very similar to that of $Zn_{0.9}Cr_{0.05}Fe_{0.05}Se$ but the important common band for the V and Co atoms around E_F is more pronounced. The local magnetic moments on the V and Co atoms were 2.16 μ_B and $-1.92\ \mu_B$, respectively. Again, induced moments on the Zn and Se atoms and the half-metallicity give zero total magnetic moment per unit cell.

In figure 4 the density of states for the III–V system $Ga_{1-2x}Mn_xCo_xAs$ with $x = 0.047$ is displayed using the PAW method and the LDA. From the counting rules it is expected that this combination of transition metals should result in an antiferromagnetic material. However, as clearly seen from the density of states the system is not at all half-metallic but rather metallic. Instead of zero total magnetic moment the system has a net magnetic moment of approximately

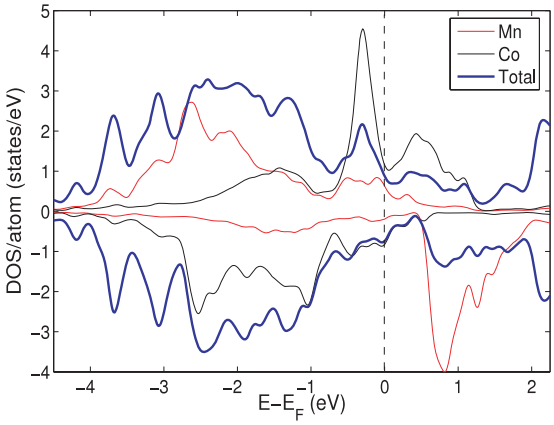

Figure 4. Density of states (DOS) of $Ga_{0.9}Mn_{0.05}Co_{0.05}As$ using the PAW method (LDA). Positive (negative) values corresponds to majority (minority) states. The total DOS has been scaled for better readability.

2 μ_B per unit cell, where the average local magnetic moment on the Mn and Co atoms were 3.43 μ_B and -1.48 μ_B, respectively. As the reason for the discrepancy between the theory and the calculations could be assigned to the local density approximation we also performed additional LDA + U calculations but still the system remained metallic. Clearly the reason for the metallic behaviour is the failure of Co impurities in GaAs to support a high-spin moment of 4 μ_B, which could compensate the 4 μ_B moment of Mn in GaAs. Indeed $Ga_{1-x}Co_xAs$ is not half-metallic. However, as was shown by Sato *et al* [31], Co in (Ga, Co)N is nearly half-metallic in the LDA calculation. Therefore we expect that in an LDA + U treatment with a reasonable U value of 3–4 eV, (Ga, Co)N would become half-metallic and as a result also $Ga_{1-2x}Mn_xCo_xN$ might be a half-metallic antiferromagnet. In order to test this concept, we did perform a LDA + U calculation ($U = 3$ eV) of $Ga_{1-2x}Mn_xCo_xN$ and indeed the system was found to be half-metallic. In the LDA, however, the system remains metallic. Similar arguments are also valid for the second candidate for half-metallic antiferromagnetism based on III–V semiconductors, i.e. $Ga_{1-2x}Cr_xNi_xAs$. The calculations give a magnetic solution, but no half-metallicity. This is in line with the observation, that Ni in (Ga, Ni)As is not magnetic at all. Therefore Ni cannot supply a spin moment of 3 μ_B necessary for half-metallicity. However, using the same arguments as above, $Ga_{0.9}Cr_{0.05}Ni_{0.05}N$ is indeed becoming a half-metallic antiferromagnet according to our calculations using a LDA + U treatment. Thus, it seems that for wide band gap semiconductors the hybridization with the valence band p states is sufficiently decreased, so that many more half-metallic antiferromagnets can exist.

3.1.2. Exchange coupling parameters. In figure 5 the calculated magnetic exchange interactions using the LSDA approximation in $Zn_{0.9}Cr_{0.05}Fe_{0.05}Se$ and $Zn_{0.9}V_{0.05}Co_{0.05}Se$ are displayed as a function of distance. Due to the half-metallicity, disorder and the fact that the important impurity bands from the magnetic atoms are situated in the band gap region, the exchange interactions are strongly damped with respect to the distance [32, 19, 20]. Furthermore, the exchange interactions are essentially non-zero only for distances shorter than 1.5 lattice constants. The exchange interactions between a Cr atom and another Cr atom are ferromagnetic, while the exchange interactions between an Fe atom and another Fe atom are weakly antiferromagnetic. The exchange interactions between a Cr atom and an Fe atom

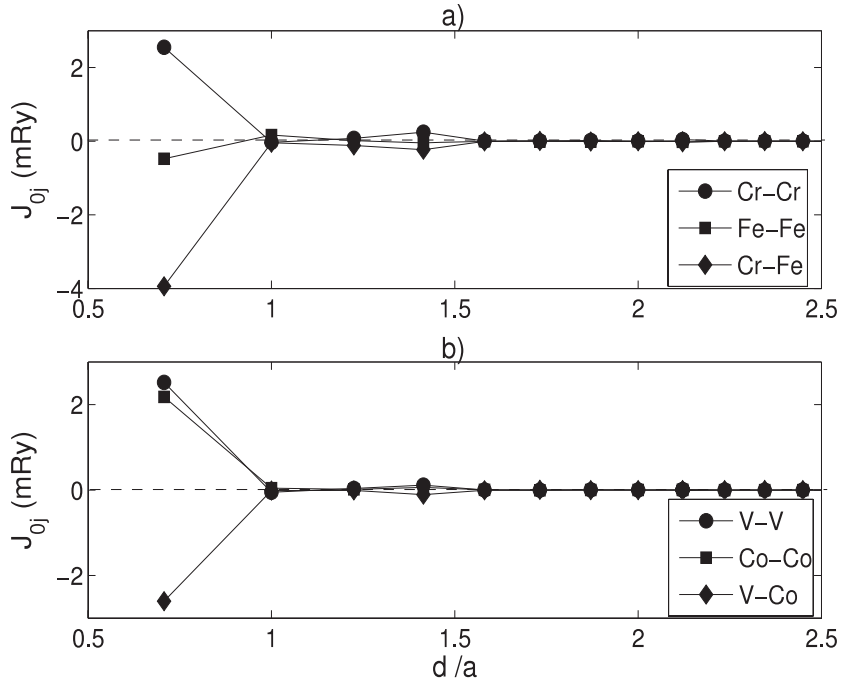

Figure 5. Exchange interactions of (a) $Zn_{0.9}Cr_{0.05}Fe_{0.05}Se$ and (b) $Zn_{0.9}V_{0.05}Co_{0.05}Se$ using the KKR-ASA–CPA method and the LSDA approximation plotted as a function of distance d (in units of the lattice constant a).

are strongly antiferromagnetic and basically determine the overall magnetic structure of the system. As discussed by Akai and Ogura, the strong antiferromagnetic Cr–Fe coupling arises from the double exchange mechanism in the joint impurity band. Since the d states of Cr in this band are mostly filled and the Fe DOS is shifted to higher energies, superexchange also plays an important role. In fact it is more or less impossible to distinguish both mechanisms in this case. The slightly negative Fe–Fe interaction is balanced by the indirect ferromagnetic Fe–Cr–Fe interaction provided by the strong antiferromagnetic interaction with the Cr atoms.

The situation in $Zn_{0.9}V_{0.05}Co_{0.05}Se$ is slightly different (figure 5(b)). Here the exchange interactions between atom components of the same type (V–V and Co–Co) are ferromagnetic with a dominating nearest neighbour interaction. The exchange interaction between V and Co is strongly antiferromagnetic. This situation can be understood from the complete overlap between the V DOS and the Co DOS, which due to double exchange leads to strong antiferromagnetic V–Co coupling and at the same time to strong ferromagnetic V–V and Co–Co coupling.

3.1.3. Critical temperatures. The critical temperatures were evaluated using the above calculated exchange parameters and then applying statistical methods. The methods used were the mean-field approximation (MFA) and the Monte Carlo (MC) simulations. It should be noticed that the MFA uses the virtual crystal approximation (VCA) to treat the disorder while the MC simulations treat the disorder exactly without any approximations using large supercells. Since the calculated exchange interactions are rather short ranged it is expected that

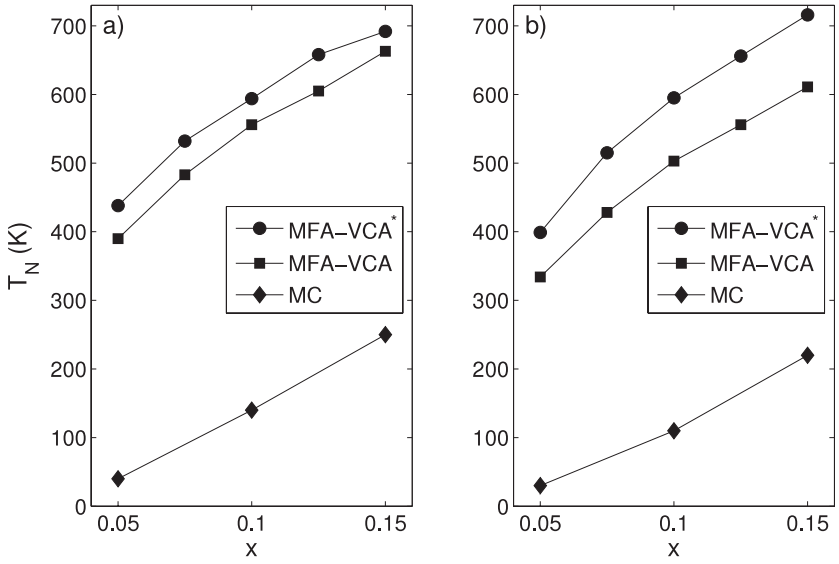

Figure 6. Calculated critical temperatures of (a) $Zn_{1-2x}Cr_xFe_xSe$ and (b) $Zn_{1-2x}V_xCo_xSe$ in K using exchange parameters from the LSDA. MFA-VCA* denotes the mean-field approximation where T_N is estimated from the total energy difference between the antiferromagnetic and DLM configuration, MFA-VCA denotes the mean-field approximation results estimated from the exchange interactions and MC the result from MC simulations.

the VCA will strongly overestimate the critical temperatures. In figure 6 the calculated critical temperatures are displayed.

Ultimately, spintronics systems should have a critical temperature well above room temperature in order to work satisfactorily in applications. The mean-field approximation give results that are above room temperature for all concentrations considered. However, the more sophisticated MC method gives much lower values for the critical temperatures. Note that for nearest neighbour interaction on a fcc lattice, which is the relevant sublattice for the transition metal impurities, the threshold for percolation is 20%. In addition, around 20% is also the practical solubility limit for transition metal atoms in II–VI compounds. Therefore, for this concentration ($x = 10\%$), the largest calculated Néel temperature of 140 K is way too low for applications.

In order to see what influence electron correlations have on the critical temperature, we performed some additional supercell calculations and calculated the energy difference between the ferromagnetic and antiferromagnetic configurations using both LSDA and LSDA + U approximations. The critical temperature is to a very crude approximation proportional to this energy difference in the mean-field approximation. The inclusion of a Hubbard U lowers this energy difference compared to the LSDA result, meaning that the expected critical temperature in LSDA + U will be lower than the LSDA results. The effect on the anion was studied by calculating T_N in the mean-field approximation for $Zn_{0.9}Cr_{0.05}Fe_{0.05}Te$ and comparing this result to $Zn_{0.9}Cr_{0.05}Fe_{0.05}Se$ given above. The overall electronic structure is similar in the two systems but ZnTe has a larger lattice parameter and smaller band gap compared to ZnSe. The critical temperature estimated from the energy difference between the antiferromagnetic and DLM state was found to 544 K in the case of ZnTe host and 437 K for the ZnSe host. However, the critical temperatures using the more exact MC method is not expected to differ much, although it will be slightly larger for the ZnTe host.

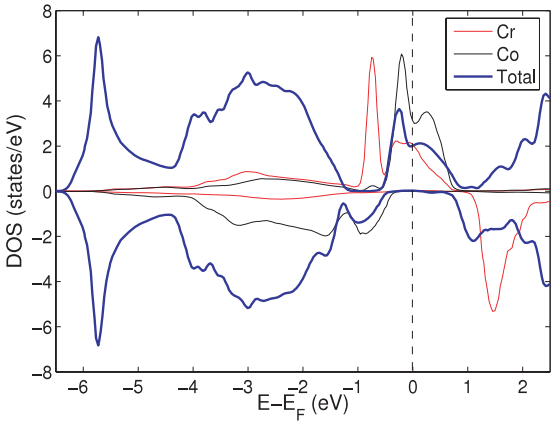

Figure 7. Total DOS of $Zn_{0.90}Cr_{0.05}Co_{0.05}Se$ using the KKR-ASA method (LDA). Positive (negative) values correspond to majority (minority) states.

3.2. Ferrimagnetic solutions

In this section we present results of combinations of magnetic atoms which give rise to a ferrimagnetic solution, i.e. the local magnetic moments do not fully compensate each other and therefore the system has a finite integer magnetic moment as discussed previously.

3.2.1. Density of states and magnetic moments. Figure 7 shows the calculated density of states $Zn_{0.9}Cr_{0.05}Co_{0.05}Se$ obtained using the KKR-CPA method. The system is half-metallic with a net magnetic moment of 1 μ_B per cell. The average local magnetic moments on the Cr and Co atoms are 3.35 μ_B and -2.10 μ_B, respectively. The total moments per impurity for the DMSs (Zn, Cr)Se and (Zn, Co)Se are 4 μ_B and 3 μ_B, respectively. The overall electronic structure is very similar to the antiferromagnetic DMS systems, but with the important difference that the system has a net magnetic moment and is ferrimagnetic.

3.2.2. Exchange interactions and critical temperatures. Using the same methodology as for the antiferromagnetic materials, we calculated the exchange interactions for the ferrimagnetic systems $Zn_{0.9}Cr_{0.05}Co_{0.05}Se$ and $Zn_{0.9}Mn_{0.05}Fe_{0.05}Se$ (figure 8). In the first case the exchange interactions are very similar to those in figure 5(b), i.e. the exchange interactions between atoms of the same type (Cr–Cr and Co–Co) are ferromagnetic while interactions between atoms of different type (Cr–Co) are antiferromagnetic. The strongest interaction is the one between Cr and Co, which controls the overall magnetic structure of the system. The situation in $Zn_{0.9}Mn_{0.05}Fe_{0.05}Se$ is rather different (figure 8(b)). Here, the exchange interactions between atoms of same type (Mn–Mn and Fe–Fe) are also antiferromagnetic. Again the largest interaction is the antiferromagnetic coupling between the Mn and Fe atoms; however, the Mn–Mn interaction is also antiferromagnetic and of nearly equal size, while the Fe–Fe interaction is very small. Clearly this is a complicated system, since the strong Mn–Fe interaction asks for an antiparallel alignment of both subsystems, while the strong antiferromagnetic Mn–Mn interaction and the weaker Fe–Fe interaction ask for disordered local moment states for the subsystems. It is therefore not clear what interaction will win.

In figure 9 we show the critical temperatures for $Zn_{0.90}Cr_{0.05}Co_{0.05}Se$ and $Zn_{0.9}Mn_{0.05}Fe_{0.05}Se$ as calculated in the mean-field approximation and by Monte Carlo simulations. Two variants of the mean-field approximation are used: the minimization of the

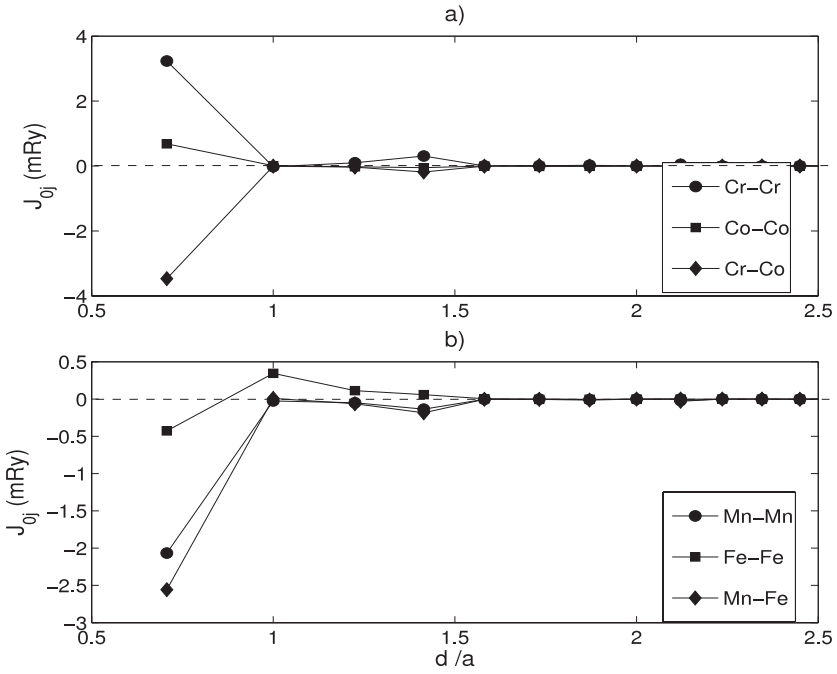

Figure 8. Exchange interactions of (a) $Zn_{0.90}Cr_{0.05}Co_{0.05}Se$ and (b) $Zn_{0.9}Mn_{0.05}Fe_{0.05}Se$ plotted as a function of distance d/a, where a is the lattice constant.

total energy within the CPA formalism indicated by MFA-VCA*, and the MFA solution of the Heisenberg model, as indicated in equations (4), (5) (MFA-VCA). For the estimation of the Curie temperatures of the ferrimagnets, Binder's cumulant expression has been used. For $Zn_{0.90}Cr_{0.05}Co_{0.05}Se$ the calculated critical temperatures are very similar to the Néel temperatures of $Zn_{0.90}Cr_{0.05}Fe_{0.05}Se$ in figure 6. In particular, the mean-field results are very high; however, the exact results obtained by Monte Carlo (MC) simulations are disappointingly low due to the percolation problem.

In $Zn_{0.9}Mn_{0.05}Fe_{0.05}Se$, the dominating antiferromagnetic interactions between all atoms makes the situation different. Here the mean-field approximation predicts finite T_N, both from total energy calculations and from the Heisenberg model (note the reduced scale in figure 9(b)). However, using the more exact Monte Carlo simulations, the system does not develop any detectable magnetic order and stays in the disordered state all the way down to zero temperature. This is plausible since the frustration inherent in the all antiferromagnetic interactions can be minimized by non-collinear moment arrangements, which cannot be described by the mean-field approximation.

4. Conclusions

In conclusion, we have given an extensive study of half-metallic antiferromagnetic diluted magnetic semiconductors using a combination of electronic structure calculations and statistical methods. The disorder of the atoms is treated carefully using both the coherent potential approximation (CPA) and large supercells. It is found that both methods give similar results for the electronic structure calculations. The calculated magnetic exchange parameters in a Heisenberg model have subsequently been used in Monte Carlo (MC) simulations to estimate

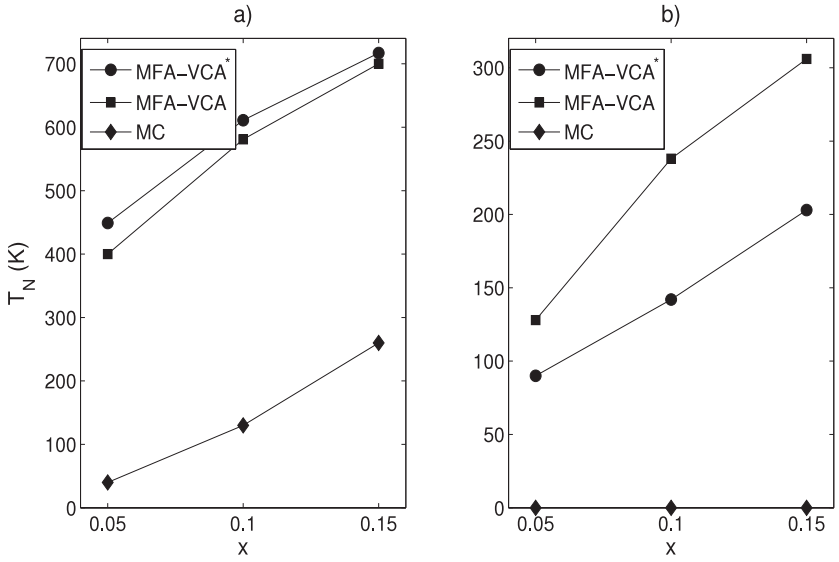

Figure 9. Calculated critical temperatures of (a) $Zn_{1-2x}Cr_xCo_xSe$ and (b) $Zn_{1-2x}Mn_xFe_xSe$ in K. MFA-VCA* denotes the mean-field approximation where T_N is estimated from the total energy difference between the antiferromagnetic and DLM configuration, MFA-VCA denotes the mean-field approximation results estimated from the exchange interactions, and MC the result from MC simulations.

critical temperatures. The MC method treats disorder exactly using very large supercells and the results from these simulations were compared to those from the mean-field approximation. It is shown that the latter method strongly overestimates the critical temperatures and that the realistic Monte Carlo values are disappointedly low. In total we have predicted quite a few half-metallic antiferromagnets and indicated that even more half-metallic ferrimagnets should exist. We hope that our results encourage experimental studies of these systems.

Acknowledgments

The authors thank H Akai and M Ogura for interesting and helpful discussions about half-metallic antiferromagnetic DMSs. Support from the John von Neumann Institut für Computing at the Forschungszentrum Jülich is acknowledged.

References

[1] Datta S and Das B 1990 *Appl. Phys. Lett.* **56** 665
[2] Prinz G 1998 *Science* **282** 1660
[3] Ohno H 1998 *Science* **281** 951
[4] Dietl T 2002 *Semicond. Sci. Technol.* **17** 377
[5] Edmonds K W, Wang K Y, Campion R P, Neumann A C, Foxon C T, Gallagher B L and Main P C 2002 *Appl. Phys. Lett.* **81** 3010
[6] Edmonds K W, Wang K Y, Campion R P, Neumann A C, Farley N R S, Gallagher B L and Foxon C T 2002 *Appl. Phys. Lett.* **81** 4991
[7] Edmonds K W, Boguslawski P, Wang K Y, Campion R P, Novikov S N, Farley N R S, Gallagher B L, Foxon C T, Sawicki M, Dietl T, Buongiorno Nardelli M and Bernholc J 2004 *Phys. Rev. Lett.* **92** 037201

[8] Theodoropoulou N, Hebard A F, Overberg M E, Abernathy C R, Pearton S J, Chu S N G and Wilson R G 2002 *Phys. Rev. Lett.* **89** 107203
[9] Reed M L, El-Masry N A, Stadelmaier H H, Ritums M E, Reed N J, Parker C A, Roberts J C and Bedair S M 2001 *Appl. Phys. Lett.* **79** 3473
[10] Ando K 2002 *Appl. Phys. Lett.* **82** 100
[11] Saito H, Zayets V, Yamagata S and Ando K 2003 *Phys. Rev. Lett.* **90** 207202
[12] Ueda K, Tabata H and Kawai T 2001 *Appl. Phys. Lett.* **79** 988
[13] Risbud A S, Spaldin N A, Chen Z Q, Stremmer S and Seshadri R 2003 *Phys. Rev.* B **68** 205202
[14] Akai H and Ogura M 2006 *Phys. Rev. Lett.* **97** 026401
[15] Leuken H and de Groot R A 1995 *Phys. Rev. Lett.* **74** 1171
[16] Pickett W E 1998 *Phys. Rev.* B **57** 10613
[17] Kresse G and Furthmüller J 1996 *Phys. Rev.* B **54** 11169
[18] Kresse G and Joubert D 1999 *Phys. Rev.* B **59** 1758
[19] Bergqvist L, Eriksson O, Kudrnovský J, Drchal V, Korzhavyi P A and Turek I 2004 *Phys. Rev. Lett.* **93** 137202
[20] Bergqvist L, Eriksson O, Kudrnovský J, Drchal V, Bergman A, Nordström L and Turek I 2005 *Phys. Rev.* B **72** 195210
[21] Bouzerar R, Bouzerar G and Ziman T 2006 *Phys. Rev.* B **73** 024411
[22] Sato K, Schweika W, Dederichs P H and Katayama-Yoshida H 2004 *Phys. Rev.* B **70** 201202(R)
[23] Korzhavyi P A, Abrikosov I A, Johansson B, Ruban A V and Skriver H L 1999 *Phys. Rev.* B **59** 11693
[24] Perdew J P, Burke K and Ernzerhof M 1996 *Phys. Rev. Lett.* **77** 3865
[25] Zunger A, Wei S H, Ferreira L G and Bernard J E 1990 *Phys. Rev. Lett.* **65** 353
[26] Liechtenstein A I, Katsnelson M I, Antropov V P and Gubanov V A 1987 *J. Magn. Magn. Mater.* **67** 65
[27] Xu J L, Schilfgaarde M and Samolyuk G D 2005 *Phys. Rev. Lett.* **94** 097201
[28] Anderson P W 1963 *Theory of Magnetic Exchange Interactions: Exchange in Insulators and Semiconductors in Solid State Physics* vol 14, ed F Seitz and D Turnbull (New York: Academic) p 99
[29] Rusz J, Bergqvist L, Kudrnovský J and Turek I 2006 *Phys. Rev.* B **73** 212412
[30] Landau D P and Binder K 2000 *A Guide to Monte Carlo Simulations in Statistical Physics* (Cambridge: Cambridge University Press)
[31] Sato K and Katayama-Yoshida H 2002 *Semicond. Sci. Technol.* **17** 367
[32] Kudrnovský J, Turek I, Drchal V, Máca F, Weinberger P and Bruno P 2004 *Phys. Rev.* B **69** 115208